

Fluoxetine inhibits transient global ischemia-induced hippocampal neuronal death and memory impairment by preventing blood–brain barrier disruption

Jee Y. Lee^{a,b}, Hyung E. Lee^d, So R. Kang^c, Hye Y. Choi^a, Jong H. Ryu^{d,**}, Tae Y. Yune^{a,b,c,e,*}

^a Age-Related and Brain Diseases Research Center, School of Medicine, Kyung Hee University, Seoul 130-701, Republic of Korea

^b Neurodegeneration Control Research Center, School of Medicine, Kyung Hee University, Seoul 130-701, Republic of Korea

^c Graduate Program for Neuroscience, School of Medicine, Kyung Hee University, Seoul 130-701, Republic of Korea

^d Department of Oriental Pharmaceutical Science, College of Pharmacy, Kyung Hee University, Seoul 130-701, Republic of Korea

^e Department of Biochemistry and Molecular Biology, School of Medicine, Kyung Hee University, Seoul 130-701, Republic of Korea

ARTICLE INFO

Article history:

Received 29 August 2013

Received in revised form

6 November 2013

Accepted 18 November 2013

Keywords:

Blood–spinal cord barrier

Matrix metalloprotease

Global ischemia

Tight junction

Hippocampus

ABSTRACT

Ischemia induces blood–brain barrier (BBB) disruption by matrix metalloproteases (MMPs) activation, leading to neuronal cell death. Here, we show that fluoxetine inhibits apoptotic cell death of hippocampal neuron and memory impairment by blocking BBB disruption after transient global ischemia. Fluoxetine treatment (10 mg/kg) after global ischemia significantly inhibited mRNA expression of MMP-2 and -9 and reduced MMP-9 activity. By Evan blue assay, fluoxetine reduced ischemia-induced BBB permeability. In parallel, fluoxetine significantly attenuated the loss of occludin and laminin in the hippocampal area after ischemia. By immunostaining with occludin antibody, fluoxetine preserved the integrity of vascular networks, especially in hippocampal areas after injury. Fluoxetine also prevented the infiltration of macrophages and inhibited the mRNA expression of inflammatory mediators after injury. In addition, the activation of microglia and astrocyte in hippocampal regions was significantly attenuated by fluoxetine. Finally, fluoxetine reduced apoptotic cell death of hippocampal neurons as well as vascular endothelial cell death and improved learning and memory. Thus, our study suggests that the neuroprotective effect of fluoxetine is likely mediated by blocking MMP activation followed BBB disruption after transient global ischemia, and the drug may represent a potential therapeutic agent for preserving BBB integrity following ischemic brain injury in humans.

© 2013 Elsevier Ltd. All rights reserved.

1. Introduction

Cerebral ischemia leads to brain injury that is induced by a complex series of pathophysiological events. After ischemic injury, primary neuronal cell death is initiated through reactive oxygen species (ROS), excitotoxicity, and Zn²⁺ toxicity, which forms the

ischemic core (Lipton, 1999), and is then followed by a second neuronal injury, called delayed neuronal death, in neighboring regions (Kirino, 2000). Particularly, neuronal cell death is prominent in the sensitive areas of brain such as the hippocampus and striatum after transient global cerebral ischemia (Kirino, 1982; Pulsinelli et al., 1982).

The blood–brain barrier (BBB) is a highly specialized brain endothelial structure in the central nervous system (CNS). The BBB is primarily formed by specialized brain endothelial cells, which form a tight seal due to the presence of well-developed tight junction that leads to limiting the entry of plasma components and blood cells into the brain. When BBB is damaged by various injury including ischemic stroke, the BBB disruption generates neurotoxic substances that lead to abnormal synaptic and neuronal functions (Hawkins and Davis, 2005; Abbott et al., 2006; Zlokovic, 2008) and to neuronal cell death (Xu et al., 2001; Noble et al., 2002; Gerzanich et al., 2009). Therefore, blocking BBB disruption can be considered as a potential therapeutic intervention after ischemic stroke. In this

Abbreviations: BBB, blood–brain barrier; CNS, central nervous system; MMP, matrix metalloprotease; Or, oriens layer; Rad, radiatum; ROS, reactive oxygen species; TUNEL, terminal deoxynucleotidyl transferase-mediated deoxyuridine triphosphate-biotin nick end labeling; tPA, tissue plasminogen activator.

* Corresponding author. Department of Biochemistry and Molecular Biology, Age-Related and Brain Diseases Research Center, School of Medicine, Kyung Hee University, Medical Building 10th Floor, #1 Hoegi-dong, Dongdaemun-gu, Seoul 130-701, Republic of Korea. Tel.: +82 02 961 0968; fax: +82 02 969 6343.

** Corresponding author. Department of Oriental Pharmaceutical Science, College of Pharmacy, Kyung Hee University, #1 Hoegi-dong, Dongdaemun-gu, Seoul 130-701, Republic of Korea. Tel.: +82 02 961 9230; fax: +82 02 966 3885.

E-mail addresses: jhyu63@khu.ac.kr (J.H. Ryu), tyune@khu.ac.kr (T.Y. Yune).

regard, it should be noted that tissue plasminogen activator (tPA), the only US FDA approved drug for treatment of acute ischemic stroke, induces MMP activation and BBB disruption (Adibhatla and Hatcher, 2008).

Matrix metalloproteases (MMPs), a family of zinc endopeptidases, are known to be involved in a variety of cellular activities such as degradation of extracellular matrix and other extracellular proteins (Sternlicht et al., 1999; Sternlicht and Werb, 2001), tissue morphogenesis and wound healing (Werb, 1997). MMPs have been considered key molecules involved in the disruption of BBB. Excessive MMP activity leads to various pathological conditions by disrupting BBB after ischemic brain injury (Rosenberg et al., 1994; Rosenberg et al., 1995; Rosenberg and Navratil, 1997; Rosenberg et al., 1998; Xu et al., 2001; Asahi et al., 2001; Noble et al., 2002). For example, MMP-2 and MMP-9 activities have been implicated specifically in BBB disruption after cerebral ischemic injury (Lo et al., 2002). MMP-9 deficient knock-out mice are more protected against brain trauma and focal cerebral ischemia than wild type mice (Wang et al., 2000; Asahi et al., 2000). MMP-9 also induces proteolytic degradation of BBB, leading to increase in an infarct volume after transient cerebral ischemia (Asahi et al., 2001). Furthermore, MMPs have been implicated in neurodegenerative disorders such as multiple sclerosis and Alzheimer's disease (Yong et al., 1998; Hartung and Kieseier, 2000).

Fluoxetine, a serotonin reuptake inhibitor as an anti-depressant drug, has been shown to provide neuroprotective effects via its anti-inflammatory effect after ischemic injury (Lim et al., 2009; Chung et al., 2011). Also, our recent report demonstrates that fluoxetine improves functional recovery by inhibiting MMPs activation and preventing blood spinal cord barrier disruption after spinal cord injury (Lee et al., 2012). Here, we examined whether fluoxetine would inhibit MMPs activation and BBB disruption, thereby attenuate neuronal cell death after transient global ischemia.

2. Materials and methods

2.1. Animals

Adult male CD1 mice (33–37 g, 8 weeks old) were purchased from the Orient Co., Ltd., a branch of Charles River Laboratories (Seoul, Korea). Animals were housed 4 per cage, allowed access to water and food ad libitum, and maintained under a constant temperature ($23 \pm 1^\circ\text{C}$) and humidity ($60 \pm 10\%$) under a 12 h light/dark cycle (light on 07:30–19:30 h). Animal treatment and maintenance were approved and conducted in accordance with the Animal Care and Use Guidelines of Kyung Hee University, Seoul, Korea.

2.2. Surgical procedure

Animals were anesthetized with isoflurane (2% for induction, 1% for maintenance) in a mixture of nitrous oxide and oxygen (70:30) and subjected to transient global ischemia as previously described (Kim et al., 2009). After making a median incision in the neck skin, both common carotid arteries were exposed and occluded with aneurysm clips for 15 min, and circulation was restored by removing the clips. Mice receiving the same surgical operation without clipping of the carotid arteries served as sham-operated controls. Throughout the surgical procedure, body temperature was maintained at $37 \pm 0.5^\circ\text{C}$ with a heating pad (Biomed S.L., Alicante, Spain). Regional cerebral blood flow was monitored using laser Doppler flowmetry (LDF; Perimed, PF5010, JarFalla, Sweden) from the time of anesthetic induction to 10 min after reperfusion. Only those mice with bilateral regional cerebral blood flow of $\leq 10\%$ of baseline were used for further study (Zhen and Dore, 2007). After reperfusion, the animals were placed in a warm incubator ($32\text{--}33^\circ\text{C}$).

2.3. Drug administration

Fluoxetine (Sigma, St. Louis, MO) dissolved in sterile PBS were immediately administered into injured mice via intraperitoneal injection (10 mg/kg) (Begovic et al., 2004; Anjaneyulu and Chopra, 2006; Sounvoravong et al., 2007) after ischemia and then further treated once a day for 1 weeks for behavioral test or for indicated time points for other experiments. PBS was administered for vehicle control. Significant side effects resulting from fluoxetine treatment such as changes in body weight or an increase in mortality were not observed throughout experiments.

2.4. Tissue preparation

Mice were anesthetized with an intramuscular injection of Zoletil 50[®] (10 mg/kg), perfused transcardially with phosphate buffer (100 mM, pH 7.4) followed by ice-cold 4% paraformaldehyde and then decapitated. The brains were removed and post-fixed overnight in phosphate buffer (50 mM, pH 7.4) containing 4% paraformaldehyde. The brains were then immersed in a 30% sucrose solution (in 50 mM phosphate-buffered saline, PBS) and stored at 4°C until sectioning. Frozen brains were sectioned along in the coronal plane (30 μm) using a cryostat (Leica Microsystems AG, Germany) and maintained in a storage solution at 4°C .

2.5. Nissl staining

After mounted onto gelatin-coated slides, tissue sections were stained with 0.5% Cresyl violet, dehydrated through graded alcohols (70%, 80%, 90%, and 100% $\times 2$), placed in xylene, and covered with a coverslip after the addition of Histomount media.

2.6. Western blot

Total protein isolated from hippocampal tissues at the indicated time point was prepared with a lysis buffer containing 50 mM Tris-HCl, pH 8.0, 150 mM NaCl, 1% NP-40, 0.5% deoxycholate, 0.1% SDS, 10 mM $\text{Na}_2\text{P}_2\text{O}_7$, 10 mM NaF, 1 $\mu\text{g}/\text{ml}$ aprotinin, 10 $\mu\text{g}/\text{ml}$ leupeptin, 1 mM sodium vanadate, and 1 mM PMSF. Tissue homogenates were incubated for 20 min at 4°C , and centrifuged at $25,000 \times g$ for 30 min at 4°C . The protein concentration was determined using the BCA assay kit (Pierce). Protein sample (40 μg) was separated on SDS-PAGE and transferred to nitrocellulose membrane (Millipore, Billerica, MA). The membranes were blocked in 5% nonfat skim milk or 5% bovine serum albumin in TBST for 1 h at room temperature followed by incubation with antibodies against occludin (1:1,000, Invitrogen, Carlsbad, CA), CD68 (ED-1, 1:500, Serotec, Raleigh, NC), GFAP (1:3,000, DAKO, Glostrup, Denmark), iNOS (1:10,000, Transduction Laboratory, Lexington, KY) and COX-2 (1:1,000, Cayman Chemicals Ann Arbor, MI). The primary antibodies were detected with horseradish peroxidase-conjugated secondary antibodies (Jackson ImmunoResearch, West Grove, PA). Immunoreactive bands were visualized by chemiluminescence using Supersignal (Thermo scientific, Rockford, IL). β -tubulin (1:20,000; Sigma) was used as an internal control. Experiments were repeated three times and the densitometric values of the bands on Western blots obtained by Alphamager software (Alpha Innotech Corporation, San Leandro, CA) were subjected to statistical analysis. Background in films was subtracted from the optical density measurements.

2.7. Gelatin zymography

The activity of MMP-2 and -9 at 7 d after injury was examined by gelatin zymography based on a previously described protocol with some modifications (Noble et al., 2002). Briefly, hippocampal tissues were weighed and homogenized in lysis buffer containing the following: 28 mM Tris-HCl, 22 mM Tris-base, pH 8.0, 150 mM NaCl, 1% Nonidet P-40, 0.5% sodium deoxycholate, and 0.1% SDS. The protein concentration of the homogenates was determined by the bicinchoninic acid method (BCA protein assay kit, Pierce, Rockford, IL). After determination of protein concentration of the homogenates, equal amounts of protein (30 μg) were loaded on a Novex 10% zymogram gel (Invitrogen, Carlsbad, CA) and separated by electrophoresis with 100 V (19 mA) at 4°C for 6 h. The gel was then incubated with renaturing buffer (2.5% Triton X-100) at room temperature for 30 min to restore the gelatinolytic activity of the proteins. After incubation with developing buffer (50 mM Tris-HCl, pH 8.5, 0.2 M NaCl, 5 mM CaCl_2 , 0.02% Brij35) at 37°C for 24 h, the gel was stained with 0.5% Coomassie blue for 60 min and then destained with 40% methanol containing 10% acetic acid until appropriate color contrast was achieved. Clear bands on the zymogram were indicative of gelatinase activity. Relative intensity of zymography (relative to sham or vehicle) was measured and analyzed by Alphamager software (Alpha Innotech Corporation, San Leandro, CA). Background was subtracted from the optical density measurements. Experiments were repeated three times and the values obtained for the relative intensity were subjected to statistical analysis.

2.8. In situ zymography

In situ zymography was performed to detect and localize enzyme activity in tissue sections as described previously (Lee et al., 2004). Brains were quickly removed without fixation and frozen at -80°C . Sections (20 μm) were cut on a cryostat and incubated at room temperature overnight in 0.05 M Tris-HCl, 0.15 M NaCl, 5 mM CaCl_2 , and 0.2 mM NaN_3 , pH 7.6, containing 40 μg of FITC-labeled gelatin (Invitrogen). The *in situ* gelatinolysis was revealed by the appearance of fluorescent brain constituents and reaction products were visualized by fluorescence microscope. However, this method detects regionally specific gelatinolytic activity but does not distinguish between MMP-2 and MMP-9.

2.9. Measurement of blood brain barrier disruption

The integrity of the BBB was investigated with Evans blue dye extravasation according to previous reports (Lee et al., 2012) with few modifications. At 7 d

after injury, 0.5 ml of 2% Evans blue dye (Sigma) solution in saline was administered intraperitoneally. Three hours later, animals were anesthetized and killed by intra-cardiac perfusion with saline. The brain was removed and homogenized in a 50% trichloroacetic acid solution. After homogenization, samples were centrifuged at $10,000 \times g$ for 10 min, supernatants were collected and its fluorescence was quantified at an excitation wavelength of 620 nm and an emission wavelength of 680 nm. Dye in samples was determined as micrograms per gram of tissue from a standard curve plotted using known amounts of dye (Chen et al., 2008).

2.10. Immunohistochemistry

Frozen sections were processed for immunofluorescence staining or double labeling with antibodies against occludin (1:100, Invitrogen), CD31 (1:200, BD Biosciences, San Jose, CA), NeuN (1:100, Millipore), myeloperoxidase (MPO, 1:100, Neomarkers, Fremont, CA), ED-1 (1:500), GFAP (1:5000, DAKO), Iba-1 (1:500, Wako Chemicals, Richmond, VA), or laminin $\alpha 4$ (1:100, Santa Cruz Biotechnology). FITC or cy3-conjugated secondary antibodies were used (Jackson ImmunoResearch, West Grove, PA). Also, nuclei were labeled with 4'-diamidino-2-phenylindole (DAPI) according to the protocol of the manufacturer (Molecular Probes, Eugene, OR). Immunohistochemistry control study was performed by omission of the primary antibodies, by replacement primary antibodies with non-immune, control antibody, and by pre-absorption with an excess (10 $\mu\text{g}/\text{ml}$) of the respective antigens. Some serial sections were also stained for histological analysis with Cresyl violet acetate. For quantitative analysis of immunofluorescence data, the area of tissue fluorescence was analyzed using Image MetaMorph software (Molecular devices, Sunnyvale, CA).

2.11. TUNEL Staining

To examine apoptotic cell death after ischemia, coronal sections (30 μm thickness) including hippocampal regions were processed for terminal deoxynucleotidyl transferase-mediated deoxyuridine triphosphate-biotin nick end labeling (TUNEL) staining using an Apoptag *in situ* kit (Chemicon International, Temecula, CA). Investigators who were blind as to the experimental conditions carried out all TUNEL analyses. TUNEL-positive cells in the hippocampal CA1 area at 7 d (total 5 sections/mouse, $n = 7$) after ischemia were counted and quantified using a 20 \times objective.

2.12. RNA Isolation and RT-PCR

Total RNA was isolated using TRIZOL Reagent (Invitrogen) and 0.5 μg of total RNA was reverse-transcribed into first strand cDNA using MMLV according to the manufacturer's instructions (Invitrogen). For PCR amplifications, the following reagents were added to 1 μl of first strand cDNA: 0.5 U taq polymerase (Takara, Kyoto, Japan), 20 mM Tris-HCl, pH 7.9, 100 mM KCl, 1.5 mM MgCl_2 , 250 μM dNTP, and 10 pmole of each specific primer. PCR conditions were as follows: denaturation at 94 $^\circ\text{C}$, 30 s, primer annealing at indicated temperature, 30 s, and amplification at 72 $^\circ\text{C}$, 30 s. The primers used for MMP-2, MMP-9, Gro- α , MIP-2 α , MCP-1, MIP-1 α , MIP-1 β , IL-1 β , IL-6, TNF- α , COX-2, iNOS and GAPDH were synthesized by the Genotech (Daejeon, Korea) and the sequences of the primers are as follows (5'-3'): MMP-2 forward, 5'-ACC ATC GCC CAT CAT CAA GT-3', reverse, 5'-CGA GCA AAA GCA TCA TCC AC-3' (348 bp, 55 $^\circ\text{C}$ for 35 cycles); MMP-9 forward, 5'-AAA GGT CGC TCG GAT GGT TA-3', reverse, 5'-AGG ATT GTC TAC TGG AGT CGA-3' (698 bp, 55 $^\circ\text{C}$ for 35 cycles); Gro- α forward, 5'-CCG AAG TCA TAG CCA CAC TCA A-3', reverse, 5'-GCA GTC GTC TCT TTC TCC GTT AC-3' (127 bp, 58 $^\circ\text{C}$ for 30 cycles); MCP-1 forward, 5'-TCA GCC AGA TGC AGT TAA CG-3', reverse, 5'-GAT CCT CTT GTA GCT CTC CAG C-3' (94 bp, 55 $^\circ\text{C}$ for 30 cycles); MIP-1 α forward, 5'-ACT GCC TGC TGC TTC TCC TAC A-3', reverse, 5'-AGG AAA ATG ACA CCT GGC TGG-3' (101 bp, 63 $^\circ\text{C}$ for 35 cycles); MIP-1 β forward, 5'-TCC CAC TTC CTG CTG TTT CTC T-3', reverse, 5'-GAA TAC CAC AGC TGG CTT GGA-3' (106 bp, 60 $^\circ\text{C}$ for 30 cycles); MIP-2 α forward, 5'-AGA CAG AAG TCA TAG CCA CTC TCA AG-3', reverse, 5'-CCT CCT TTC CAG GTC AGT TAG C-3' (125 bp, 55 $^\circ\text{C}$ for 30 cycles); TNF- α forward, 5'-CCG AGA CCC TCA CAC TCA GAT-3', reverse, 5'-TTG TCC CTT GAA GAG AAC CTG-3' (215 bp, 56 $^\circ\text{C}$ for 28 cycles); IL-1 β forward, 5'-GCA GCT ACC TAT GTC TTG CCC GTG-3', reverse, 5'-GTC GTT GCT TGT CTC TCC TTG TA-3' (289 bp, 50 $^\circ\text{C}$ for 30 cycles); IL-6 forward, 5'-AAG TTT CTC TCC GCA AGA TAC TTC CAG CCA-3', reverse, 5'-AGG CAA ATT TCC TGG TTA TAT CCA GTT-3' (240 bp, 58 $^\circ\text{C}$ for 30 cycles); COX-2 forward, 5'-CCA TGT CAA AAC CGT GGT GAA TG-3', reverse, 5'-ATG GGA GTT GGG CAG TCA TCA G-3' (374 bp, 55 $^\circ\text{C}$ for 28 cycles); iNOS forward, 5'-CTC CAT GAC TCT CAG CAC AGA G-3', reverse, 5'-GCA CCG AAG ATA TCC TCA TGA T-3' (401 bp, 56 $^\circ\text{C}$ for 25 cycles); GAPDH forward, 5'-AAC TTT GGC ATT GTG GAA GG-3', reverse, 5'-GGA GAC AAC CTG GTC CTC AG-3' (351 bp, 58 $^\circ\text{C}$ for 23 cycles). The plateau phase of the PCR reaction was not reached under these PCR conditions. After amplification, PCR products were subjected to a 1.5–2% agarose gel electrophoresis and visualized by ethidium bromide staining. The relative density of bands (relative to sham value) was analyzed by the AlphaImager software (Alpha Innotech Corporation). Experiments were repeated three times and the values obtained for the relative intensity were subjected to statistical analysis. The gels shown in figures are representative of results from three separate experiments.

2.13. Y-maze task

To examine hippocampal-dependent short-term memory at 7 d after transient global ischemia, a Y-maze task was performed. The Y-maze is a three-arm horizontal maze (40-cm long and 3-cm wide with 12-cm high walls) in which the arms are at 120 $^\circ$ angles from each other. The maze floor and walls were constructed from dark opaque polyvinyl plastic as previously described (Kim et al., 2009). Animals were initially placed within one arm, and the sequence (i.e., ABCBAC) and the number of arm entries were recorded manually for each animal for 8-min period. A spontaneous alternation was defined as entries into all three arms on consecutive choices (i.e., ABC, CAB, or BCA, but not BAB). Maze arms were thoroughly cleaned with water between animals to remove residual odors. Thirty minutes after the last administration of each drug or vehicle, mice were gently placed in the maze. The percentage of alternations was defined according to the following equation: % Alternation = [(Number of alternations)/(Total arm entries - 2)] \times 100. The number of arm entries serves as an indicator of locomotor activity.

2.14. Statistical analysis

Data are presented as the mean \pm SD. Multiple comparisons between groups were performed one-way and the Student–Newman–Keuls test was used for post hoc comparisons. Statistical significance was accepted with $p < 0.05$. Statistical analyses were performed using SPSS 15.0 (SPSS Science, Chicago, IL).

3. Results

3.1. Fluoxetine reduces the expression and activation of MMP-2, and -9 after transient global ischemia

Mice were subjected to transient global ischemia and sacrificed at 3 d after injury. Total RNA and tissue extracts from hippocampal region were prepared as described above. First, we examined MMP-2 and -9 mRNA expressions after injury by RT-PCR ($n = 3$). As shown in Fig. 1A and B, mRNA levels of MMP-2 and -9 were increased after injury. Fluoxetine significantly reduced MMP-2 and MMP-9 mRNA expression at 3 d after injury as compared to vehicle control (Fig. 1A and B). Next, we analyzed MMP-2 and -9 activities by gelatin zymography. As shown in Fig. 1C and D, MMP-9 activity was markedly increased at 3 d after injury as compared with control. Furthermore, fluoxetine significantly attenuated the level of active MMP-9 as compared to vehicle control ($n = 4$, active MMP-9, Vehicle, 3.6 ± 0.46 vs. Fluoxetine, 1.4 ± 0.16 , $p < 0.05$) (Fig. 1C and D). However, fluoxetine treatment showed no significant effect on the level of MMP-2 activity in gelatin zymography (Fig. 1C). By *in situ* zymography, fluoxetine markedly inhibited gelatinolytic activity at 3 d after injury as compared to vehicle control (Fig. 1E). It should be noted that gelatinolytic activity was mainly localized in CA1 area in the hippocampus after injury (Fig. 1E). Double labeling showed that gelatinase activity was co-localized in NeuN-positive neurons in the pyramidal cell layer of hippocampal CA1 (Fig. 1F upper panel). Also, gelatinase activity was observed in blood vessels in the oriens layer (Or) and radiatum (Rad) layer of hippocampal CA1, which was co-localized with CD31 antibody, a blood vessel marker, (Fig. 1F bottom panel). Our data thus indicate that fluoxetine reduces MMP activation after ischemic injury.

3.2. Fluoxetine attenuates transient global ischemia-induced BBB permeability

It is well known that the BBB disruption occurs after ischemic injury and play important roles in pathological process leading to secondary injury (Preston and Webster, 2004; Yang et al., 2007a; Baumann et al., 2009; Liu et al., 2012). The BBB disruption by MMP activation is also well documented in various neurodegenerative animal models including ischemic and spinal cord injury (SCI) (Noble et al., 2002; Jin et al., 2010; Ramos-Fernandez et al., 2011; Lee et al., 2012; Lakhan et al., 2013). Since fluoxetine inhibited MMP expression and activation after ischemic injury (Fig. 1), we expected that fluoxetine would inhibit the injury-induced BBB permeability. Thus, we examined the effect of fluoxetine on BBB

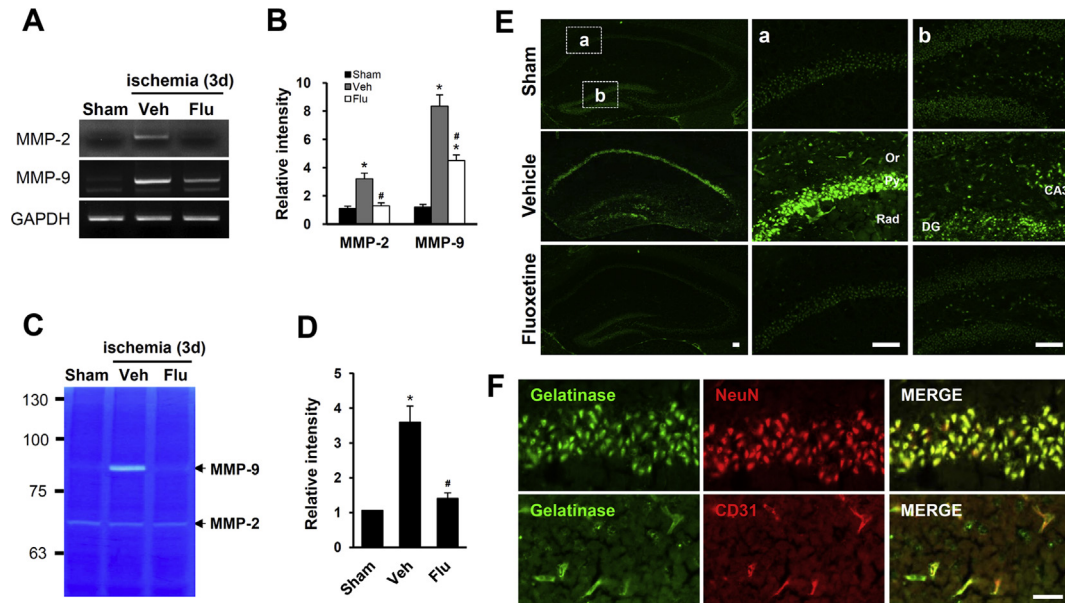


Fig. 1. Fluoxetine reduces the expression and activation of MMP-2 and -9 after transient global ischemia. After ischemic injury, fluoxetine (10 mg/kg) was administered immediately via intraperitoneal injection (i.p.) and further treated once a day for 3 d ($n = 3$). Hippocampal tissue was prepared as described in the Method. **(A)** RT-PCR of MMP-2 and -9. **(B)** Densitometric analyses of RT-PCR ($n = 3$). **(C)** Gelatin zymography. **(D)** Densitometric analyses of zymography ($n = 4$). Note that fluoxetine significantly inhibits MMP-2 and -9 mRNA expression and activation after injury as compared to vehicle control. Data represent mean \pm SD. * $p < 0.05$ vs. sham group; # $p < 0.05$, vs. vehicle-treated ischemic control group. **(E)** Representative *in situ* gelatin zymograms in the hippocampus after transient global ischemia. Gelatinase activity was up-regulated mainly in CA1 and/or CA3 areas. **(a and b)** Higher power views of CA1 (a) and CA3 (b). Or; oriens layer, Rad; stratum radiatum. Scale bars, 100 μ m. **(F)** Double staining showing cellular distributions of gelatinolytic activity in hippocampal CA1 area. Gelatinolytic activity (green fluorescence) co-localizes with NeuN-positive neurons (upper panel) and CD31-positive blood vessels (lower panel). Scale bar, 50 μ m.

permeability at 7 d after injury by Evans blue assay. As shown in Fig. 2, ischemic injury caused a marked increase in the amount of Evans blue dye extravasation as compared with sham control, which implies BBB disruption after injury. Furthermore, fluoxetine (10 mg/kg) treatment significantly reduced the amount of Evans blue dye extravasation when compared with vehicle control ($n = 5$, Vehicle, 6.0 ± 0.4 vs. Fluoxetine, 3.6 ± 0.5 , $p < 0.05$) (Fig. 2B). These data indicate that fluoxetine inhibit BBB disruption after ischemic injury.

3.3. Fluoxetine prevents loss of laminin and tight junction protein in hippocampus after transient global ischemia

Since we showed that fluoxetine inhibited BBB disruption after ischemic injury (Fig. 2), we next examined whether the drug would also inhibit the loss of tight junction and extracellular proteins by immunohistochemistry and Western blot. It is well known that laminin is distributed mainly to pyramidal cell layer and degraded markedly in the medial portion of CA1 and CA2 areas after ischemia (Lee et al., 2009). Brain tissues and hippocampal extracts from mice treated with fluoxetine at 7 d after injury were prepared as described in the Method. As shown in Fig. 3A and B, the fluorescence intensity of laminin, an extracellular protein, in hippocampal CA1 and CA2 areas after ischemia was significantly reduced as compared to sham control ($n = 3$, Vehicle, 0.47 ± 0.07 vs. Fluoxetine, 0.85 ± 0.1 , $p < 0.05$). Western blot and quantitative analysis also showed that laminin loss in hippocampus after injury was significantly attenuated by fluoxetine treatment as compared to vehicle control ($n = 3$, Vehicle, 0.65 ± 0.09 vs. Fluoxetine, 0.95 ± 0.08 , $p < 0.05$) (Fig. 3C and D). The tight junction (TJ) in the endothelial cells of blood vessels in the CNS is essential for BBB integrity (Zlokovic, 2008). To determine whether ischemia-induced hyperpermeability was due to TJ alterations, the expression of the TJ-associated protein, occludin was examined after injury. As shown in Fig. 3E, the level of occludin (65 kDa) was dramatically decreased after ischemia. Furthermore,

fluoxetine treatment significantly attenuated the decrease in occludin level as compared with vehicle control at 7 d after injury ($n = 3$, Vehicle, 0.37 ± 0.05 vs. Fluoxetine, 0.85 ± 0.07 , $p < 0.05$) (Fig. 3F and G). By immunostaining using occludin antibody, the fluorescence intensity of vascular networks in hippocampal areas was decreased after ischemia (Fig. 3G and F), which was significantly attenuated by fluoxetine treatment ($n = 3$, Vehicle, 0.3 ± 0.04 vs. Fluoxetine, 0.94 ± 0.08 , $p < 0.05$) (Fig. 3F). These data indicate that fluoxetine preserves tight junction integrity by inhibiting degradation of TJ molecules, and thereby prevents BBB disruption after transient global ischemia.

3.4. Fluoxetine inhibits macrophage infiltration after transient global ischemia

It is known that blood cell infiltration following BBB disruption after ischemia initiates inflammatory responses, leading to the secondary injury cascade by producing inflammatory mediators (Mun-Bryce and Rosenberg, 1998). Therefore, we examined the effect of fluoxetine treatment on the blood cells infiltration by Western blot and immunofluorescence staining with macrophage/monocyte cell marker, ED-1 antibody. Immunofluorescence staining showed that numerous ED-1 positive cells were observed in pyramidal layer and stratum radiatum of hippocampus at 7 d after ischemia, whereas no ED-1 positive cells were observed in sham control (Fig. 4A). Furthermore, the fluorescence intensity and the number of ED-1 positive cells were dramatically decreased in fluoxetine-treated groups as compared with vehicle control ($n = 3$, Vehicle, 6.4 ± 0.9 vs. Fluoxetine, 1.8 ± 0.4 , $p < 0.05$) (Fig. 4A and B). By Western blotting and quantitative analysis, the level of ED-1 was markedly increased after ischemia, which was significantly attenuated by fluoxetine treatment ($n = 3$, Vehicle, 2.8 ± 0.22 vs. Fluoxetine, 1.44 ± 0.15 , $p < 0.05$) (Fig. 4C and D). These results thus indicate that fluoxetine inhibits macrophage infiltration after ischemic injury by preserving BBB integrity.

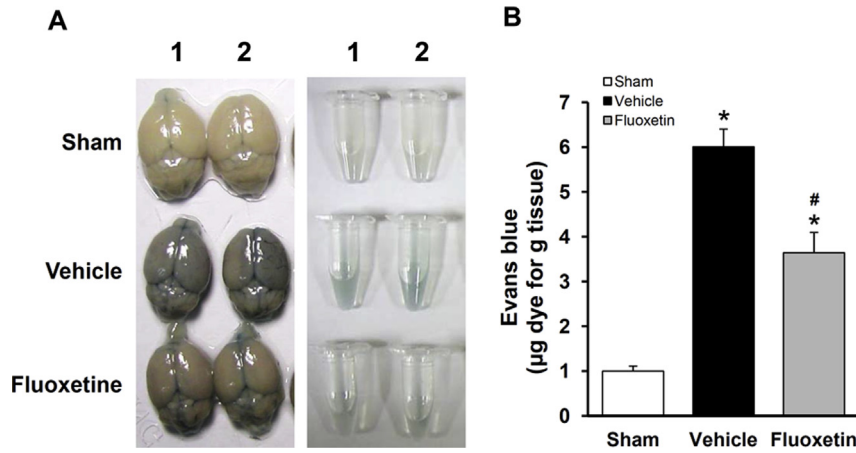


Fig. 2. Fluoxetine prevents the increase in BBB permeability after transient global ischemia. After ischemia, mice were treated with fluoxetine and BBB permeability was measured at 7 d after injury by using Evans blue dye as described in the Method ($n = 5$). **(A)** Representative whole brains (duplicates) showing Evan’s blue dye permeabilized into the brain after ischemic injury. **(B)** Quantification of the amount of Evans blue. Note that fluoxetine significantly attenuates the increase in Evans blue extravasated after injury as compared to vehicle control. Data represent mean \pm SD. * $p < 0.05$ vs. sham group; # $p < 0.05$, vs. vehicle-treated ischemic control group. (For interpretation of the references to color in this figure legend, the reader is referred to the web version of this article.)

3.5. Fluoxetine inhibits microglia and astrocyte activation after transient global ischemia

Microglia and astrocyte are activated after ischemia, mediating secondary pathological processes including inflammation (Xuan

et al., 2012; Okuyama et al., 2013; Tulsulkar and Shah, 2013). Also, fluoxetine is known to have anti-inflammatory effect in middle cerebral artery occlusion injury model (Lim et al., 2009). Thus, we postulated that fluoxetine would inhibit microglia and astrocyte activation in the hippocampus after transient global

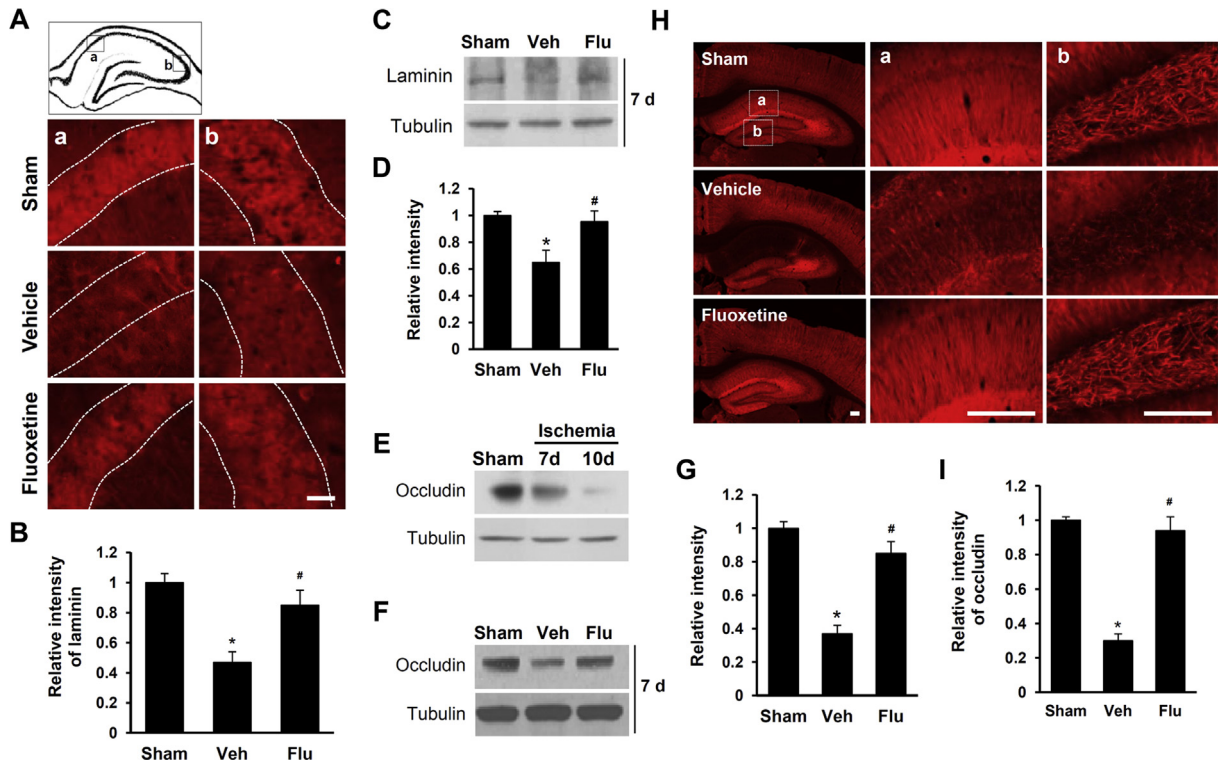


Fig. 3. Fluoxetine inhibits laminin and occludin loss in hippocampus after ischemia. Brain tissues and hippocampal extracts from mice treated with fluoxetine at 7 d after injury were prepared as described in the Method ($n = 3$). **(A)** Immunofluorescence staining showing laminin loss in the hippocampal CA1 (a) and CA2 (b) areas after injury. Scale bar, 10 μ m. **(B)** Quantitative analysis shows that the fluorescence intensity of laminin in the CA1 and CA2 was significantly reduced in fluoxetine-treated mice when compared to that in vehicle-treated mice ($n = 3$). **(C)** Western blot of laminin. **(D)** Densitometric analyses of Western blot. **(E and F)** Western blots showing temporal loss of occludin at 7 and 10 d after injury **(E)** and the effect of fluoxetine treatment on occludin loss at 7 d after injury **(F)**. **(G)** Densitometric analyses of Western blots **(F)**. **(H)** Representative fluorescence photographs showing vascular network in hippocampal region, which is labeled with occludin antibody. Note that fluoxetine significantly attenuates occludin loss in hippocampus as compared to vehicle control. **(a and b)** Higher power views of CA1 (a) and dentate gyrus (b). Scale bars, 200 μ m. **(I)** Quantitative analysis shows that the fluorescence intensity of occludin in hippocampus was significantly reduced in fluoxetine-treated mice when compared to that in vehicle-treated mice. All data represent as mean \pm SD. * $p < 0.05$ vs. sham group; # $p < 0.05$, vs. vehicle-treated ischemic control group.

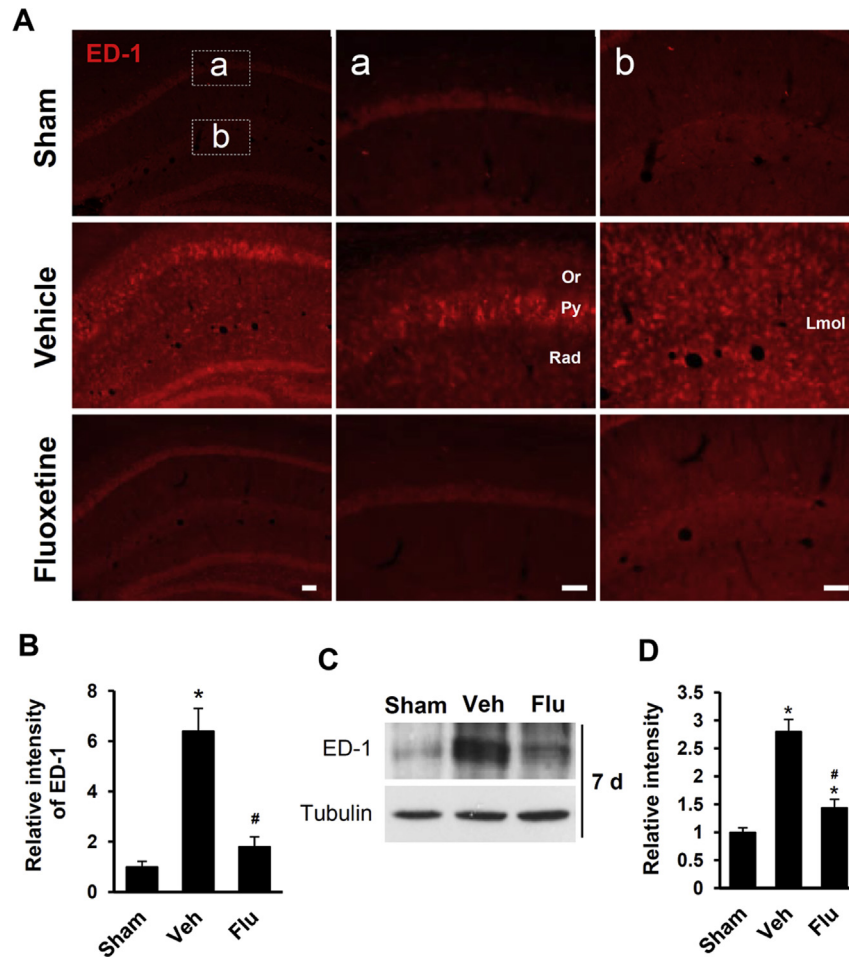


Fig. 4. Fluoxetine inhibits macrophages infiltration after ischemic injury. Brain tissue and hippocampal extracts from mice treated with fluoxetine were prepared at 7 d after injury as described in the Method ($n = 3$). **(A)** Representative fluorescence photographs showing ED-1-labeled macrophages in hippocampal areas. **(a and b)** high power views of (a) and (b). Or, oriens layer. Py, pyramidal layer. Rad, stratum radiatum. Lmol, lacunosum-molecular layer. Scale bars, 100 μm . **(B)** Quantitative analysis shows that the fluorescence intensity of ED-1 in hippocampus was significantly reduced in fluoxetine-treated mice when compared to that in vehicle-treated mice. **(C)** Western blots of ED-1 with hippocampal extracts. **(D)** Densitometric analyses of Western blots. Note that fluoxetine significantly prevents macrophage infiltration into hippocampal region after ischemia as compared with sham control. Data represent mean \pm SD. * $p < 0.05$ vs. sham group; # $p < 0.05$, vs. vehicle-treated ischemic control group.

ischemia. As shown in Fig. 5A and B, immunostaining with Iba-1 antibody, a microglia marker, revealed that numerous activated microglia were observed in pyramidal layer (Py), stratum radiatum (Rad), oriens layer (Or) and lacunosum-molecular layer (Lmol) in hippocampus CA1 area at 7 d after injury whereas fluoxetine treatment markedly reduced the number of activated microglia ($n = 3$, Vehicle, 8.6 ± 0.5 vs. Fluoxetine, 1.9 ± 0.6 , $p < 0.05$). In addition, GFAP immunofluorescence staining showed that astrocytes were also activated in the hippocampal areas after injury and ischemia-induced astrocyte activation was significantly inhibited by fluoxetine ($n = 3$, Vehicle, 7.8 ± 0.7 vs. Fluoxetine, 2.4 ± 0.4 , $p < 0.05$) (Fig. 5C and D). By Western blotting and quantification analysis, fluoxetine treatment significantly reduced the level of GFAP, which was increased after ischemia ($n = 3$, Vehicle, 5.5 ± 0.45 vs. Fluoxetine, 3.1 ± 0.24 , $p < 0.05$) (Fig. 5E and F). These results indicate that fluoxetine inhibits microglia and astrocyte activation in the hippocampus after ischemia.

3.6. Fluoxetine inhibits the expression of proinflammatory mediators and chemokines after transient global ischemia

It is known that inflammatory cytokines such as TNF- α and IL-1 β are produced after ischemic injury (Sairanen et al., 2001; Xuan

et al., 2012). The expression of chemokines such as MCP-1 (CCL-2) and MIP-1 α (CCL-3) is also known to increase after ischemia (Sakurai-Yamashita et al., 2006; Lakhani et al., 2009). Since our data showed that fluoxetine reduced macrophage infiltration and inhibited microglia and astrocyte activation after ischemia, we expected that fluoxetine would inhibit the expression of inflammatory mediators after ischemia. As shown in Fig. 6A and B, the expression of inflammatory mediators such as TNF- α , IL-1 β , IL-6, COX-2 and iNOS and chemokines such as Gro- α (CXCL-1), MCP-1, MIP-1 α , MIP-1 β (CCL-4), and MIP-2 α (CXCL-2) mRNA expression was markedly increased after ischemia as compared with sham control ($n = 3$). Furthermore their levels were decreased by fluoxetine as compared with vehicle. By Western blotting, ischemia-induced up-regulation of COX-2 and iNOS expression was significantly attenuated by fluoxetine ($n = 3$) (Fig. 6C and D). These data suggest that fluoxetine inhibits ischemia-induced inflammatory mediators and chemokines expression.

3.7. Fluoxetine inhibits hippocampal cell loss after transient global ischemia

It is well known that neuronal cell death occurs in the brain such as the hippocampus and striatum after transient global cerebral

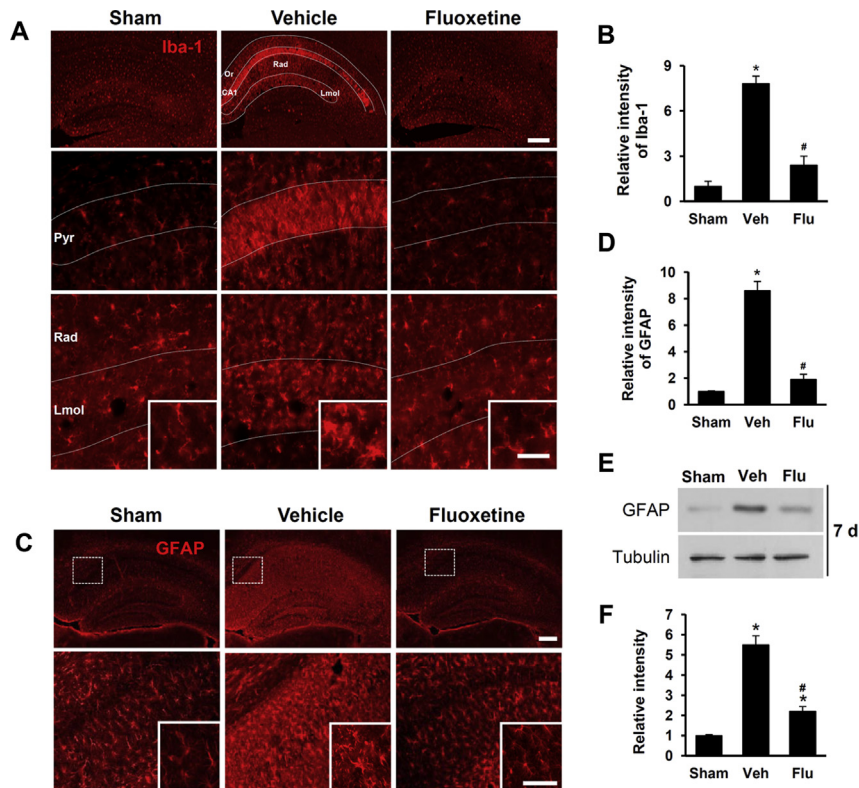


Fig. 5. Fluoxetine inhibits microglia and astrocyte activation in hippocampus after transient global ischemia. At 7 d after injury, brain tissues and hippocampal extracts were prepared as described in the Method and performed immunostaining and western blot with microglial cell marker, Iba-1 and astrocyte cell marker, GFAP antibodies ($n = 3$). **(A)** Representative photographs of Iba-1 immunofluorescence staining showing the hippocampal area (upper panel, low power views; lower panel, high power views). Dotted line indicates pyramidal layer (Pyr), stratum radiatum (Rad), oriens layer (Or) and lacunosum-molecular layer (Lmol) in hippocampus CA1 area. Inserted boxes in lower panel show higher power views of Iba-1-positive activated microglia. Scale bars, 100 μ m (Inserted box, Scale bar, 10 μ m). **(B)** Quantitative analysis shows that the fluorescence intensity of Iba-1 in hippocampus was significantly reduced in fluoxetine-treated mice when compared to that in vehicle-treated mice. **(C)** Representative photographs of GFAP immunofluorescence staining showing the hippocampal area (upper panel, low power views; bottom panel; high power views of dotted boxes in upper panel). Inserted boxes in lower panel show higher power views of GFAP-positive activated astrocytes (arrows). Scale bar, 100 μ m (Inserted box, Scale bar, 20 μ m). **(D)** Quantitative analysis shows that the fluorescence intensity of GFAP in hippocampus was significantly reduced in fluoxetine-treated mice when compared to that in vehicle-treated mice. **(E)** Western blots of GFAP. **(F)** Densitometric analyses of Western blots. Note that fluoxetine inhibits microglia and astrocyte activation in hippocampal areas after ischemia as compared with vehicle control, when evaluated by morphological features and quantitative analysis. Data represent mean \pm SD. * $p < 0.05$ vs. sham group; # $p < 0.05$, vs. vehicle-treated ischemic control group.

ischemia (Kirino, 1982; Pulsinelli et al., 1982). Since we showed inhibition of BBB disruption by fluoxetine after ischemic injury, we postulated that the drug would inhibit hippocampal cell loss after injury. By Nissl staining, the numbers of pyramidal neurons in the hippocampus CA1 region at 7 d were diminished dramatically after ischemia, whereas the loss of hippocampal neurons was attenuated by fluoxetine treatment (Fig. 7A). Quantitative analysis revealed that the number of viable pyramidal neurons in CA1 was decreased up to 20% of sham group after injury and fluoxetine treatment significantly attenuated its loss ($n = 3$, Vehicle, 25 ± 5.1 vs. Fluoxetine, 73 ± 4.0 , $p < 0.05$) (Fig. 7B).

To determine whether hippocampal neuron loss after injury was mediated by apoptotic cell death, TUNEL-staining was performed. As shown in Fig. 7C, TUNEL-positive cells were mainly observed in the hippocampal CA1 area after ischemia. However, when compared with vehicle control, TUNEL-positive cells were rarely observed in fluoxetine-treated group. Quantitative analysis showed that the number of TUNEL-positive cells in the hippocampal CA1 area in the fluoxetine-treated group was significantly lower than in vehicle control ($n = 3$, Vehicle, 73 ± 5.2 vs. Fluoxetine, 5 ± 1.5 , $p < 0.05$) (Fig. 7D). These data indicate that fluoxetine prevents hippocampal neuron loss mediated by apoptotic cell death after ischemia. As shown in Fig. 8, we also observed that fluoxetine inhibited apoptotic cell death of endothelial cells of blood vessels in the hippocampus after transient global ischemia. Several TUNEL-

positive cells were observed in blood vessels in the hippocampal areas after injury (Fig. 8, Vehicle). Double staining revealed that TUNEL-positive cells were positive for CD31 antibody, a marker of blood vessel endothelial cell (Fig. 8, Vehicle). However, TUNEL-positive cells were not observed in the fluoxetine-treated group (Fig. 8, Fluoxetine). These results thus suggest that fluoxetine also inhibits endothelial cell death in the hippocampus after ischemia.

3.8. Fluoxetine alleviates memory impairment induced by transient global ischemia

It is well known that transient global ischemia induces memory impairment due to neuronal cell loss in the hippocampus. Since we showed that fluoxetine inhibited hippocampal neuronal cell loss, we expected that fluoxetine would attenuate memory loss and learning impairment after injury. Y-maze task was conducted with mice treated with vehicle or fluoxetine at 7 d after injury. The spontaneous alternation of vehicle control in the Y-maze task was significantly shorter than that of the sham group [$F(3, 17) = 7.96$, $p < 0.05$] (Fig. 9A). In addition, ischemia-induced shorter spontaneous alternation was significantly reversed by fluoxetine treatment ($n = 10$, Vehicle, 46.1 ± 2.6 vs. Fluoxetine, 67.5 ± 2.1 , $p < 0.05$). However, any significant difference in the total number of entries was not observed among all groups (Fig. 9B and D). As a therapeutic window, significant memory improvement by fluoxetine was

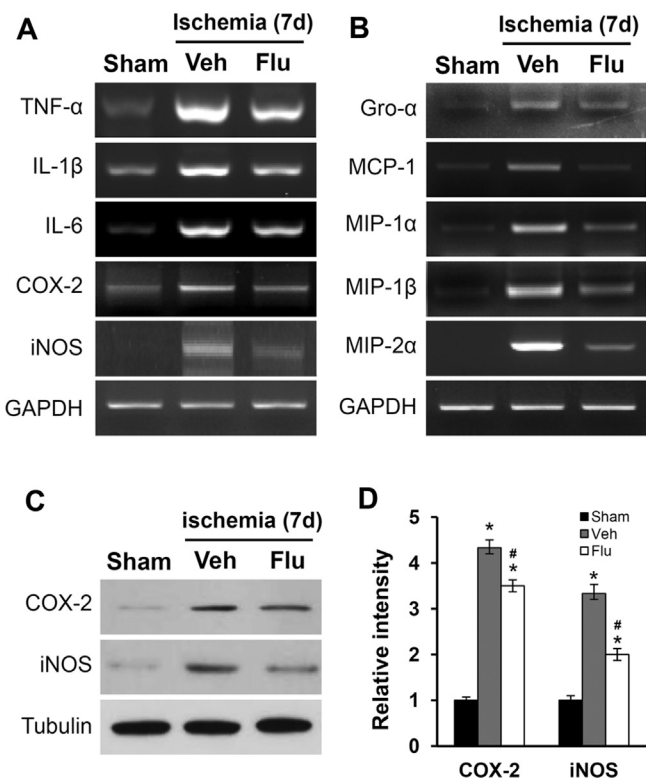


Fig. 6. Fluoxetine inhibits the expression of inflammatory mediators and chemokines after transient global ischemia. Total RNA and protein extracts from vehicle or fluoxetine-treated hippocampal tissues at 7 d after injury were prepared as described in the Method ($n = 3$). (A–B) RT-PCR of TNF- α , IL-1 β , IL-6, COX-2 and iNOS (A) and chemokines such as Gro- α , MCP-1, MIP-1 α , MIP-1 β , and MIP-2 β mRNA expression (B) in sham, vehicle-treated and fluoxetine-treated hippocampal tissues. (C) Western blots of iNOS and COX-2. (D) Densitometric analyses of Western blots. Note that fluoxetine significantly inhibits the expression of inflammatory mediators and chemokines after transient global ischemia as compared with vehicle control. Data represent mean \pm SD. * $p < 0.05$ vs. sham group; # $p < 0.05$, vs. vehicle-treated ischemic control group.

observed when the drug was treated at 0, 1, 2, 3 and 6 h after ischemia (Fig. 9C), whereas significant memory improvement was not observed at 12 h after injury ($n = 10$, Vehicle, 46.4 ± 2.7 ; Fluoxetine 0 h, 68.3 ± 3.1 ; Fluoxetine 1 h, 63.2 ± 3.4 ; Fluoxetine 2 h, 65.6 ± 2.5 ; Fluoxetine 3 h, 64.2 ± 4.1 ; Fluoxetine 6 h, 61.5 ± 4.4 ; Fluoxetine 12 h, 51.1 ± 3.8 ; $p < 0.05$). By Nissl staining, the loss of pyramidal neurons in the hippocampus CA1 region at 7 d was also attenuated by fluoxetine when it was injected at 0, 1, 2, 3, and 6 h after injury as compared with those of the vehicle-treated control (Fig. 9E). Our data indicate that fluoxetine alleviates memory impairment by inhibiting the loss of hippocampal neurons after ischemic injury.

4. Discussion

In the present study, we showed that fluoxetine, an anti-depressant drug, alleviated ischemic injury-induced memory impairment by preventing apoptotic cell death of hippocampal neurons, specifically CA1 pyramidal neurons via reducing MMPs activation and BBB disruption after transient global ischemia. Fluoxetine also reduced the number of infiltrating macrophage after injury and inhibited the expression of inflammatory mediators including pro-inflammatory cytokines and chemokines. Furthermore, we found that fluoxetine reduced degradation of occludin, a tight junction protein and laminin by reducing the activation of MMP-2 and -9, resulting in decreased BBB disruption. Our findings thus have important implications in traumatic and

ischemic brain injuries in which the disruption of BBB integrity triggers secondary degenerative cascades including inflammation and neuronal cell death in its pathological processes (Yang et al., 2007b; Yu et al., 2008; Cui et al., 2010; Higashida et al., 2011; Hosokawa et al., 2011; Miyazaki et al., 2011; Liu et al., 2012). Furthermore, the efficacy of fluoxetine for preventing the BBB disruption can be considered as a potential therapeutic application in ischemic stroke.

The BBB represents a tight barrier between the circulating blood and CNS parenchyma and is formed by tight junction proteins, which seal the space between adjacent brain endothelial cells. Under pathological conditions including ischemic stroke, the BBB integrity is disrupted, leading to an increased BBB permeability (Utepergenov et al., 1998). Furthermore, MMPs play a critical role in the BBB disruption in the pathological conditions (Asahi et al., 2001; Rosenberg, 2002; Jin et al., 2011). In the present study, our data show that fluoxetine inhibited the expression and activity of MMP-2 and/or -9, which were up-regulated after transient global ischemia (see Fig. 1). Particularly, MMP-9 activity was significantly attenuated by fluoxetine (see Fig. 1C and D). The tight junction proteins such as occludin, claudin-5, and ZO-1, are essential components of BBB and known to be substrates of MMPs (Yang et al., 2007b). Our data show that the level of occludin was decreased after ischemia (see Fig. 3E) and fluoxetine inhibited the degradation of this protein (see Fig. 3F and G). Our results thus are in agreement with that BBB disruption induced by transient focal cerebral ischemia is attenuated in MMP-9 knockout mice by reducing degradation of ZO-1 protein as compared to wild type mice (Asahi et al., 2001). MMP-9 is also known to mediate hypoxia-induced vascular leakage in the brain via tight junction rearrangement (Bauer et al., 2010). Thus, our data suggest that fluoxetine prevents BBB disruption in part by inhibiting the expression and activity of MMP-2 and/or MMP-9 after global ischemia.

MMPs including MMP-2 and -9 are known to degrade extracellular matrix of cerebral blood vessel basal lamina such as collagen type IV (Fujimoto et al., 2008). The levels of tight junction proteins such as ZO-1 and claudin-5 also decrease after ischemic injury (Fujimoto et al., 2008). In addition, MMP-9 knock-out reduces the expression of degraded ZO-1 and BBB disruption after cerebral ischemia (Asahi et al., 2001). Furthermore, MMP inhibitors reverse the degradation of tight junction proteins such as occludin and claudin-5, in focal ischemia (Yang et al., 2007b; Fujimoto et al., 2008). In our global ischemic model, fluoxetine attenuated the loss of laminin and occludin (see Fig. 3). Fluoxetine also decreases the degradation of tight junction proteins including ZO-1 and occludin by inhibiting both MMP-2 and MMP-9 activation after spinal cord injury (SCI) (Lee et al., 2012). Thus, our data suggest that the inhibition of extracellular matrix and tight junction protein degradation by fluoxetine may be attributed to the inhibition of MMPs activation.

We also found that TUNEL-positive cells were observed in the blood vessels as well as CA1 region in the hippocampal areas after ischemic injury (see Fig. 8). With double labeling, TUNEL-positive cells were positive for CD31 antibody, a blood vessel marker, indicating that endothelial cells of blood vessels were undergoing apoptotic cell death after ischemia. However, no TUNEL- and CD31-positive endothelial cells were observed in the fluoxetine-treated group (see Fig. 8). Our results thus indicate that fluoxetine inhibits apoptotic cell death of endothelial cells of blood vessels and thereby further blocking BBB disruption in the hippocampal area after ischemic injury.

Tissue plasminogen activator (tPA) is a protein involved in the breakdown of blood clots and the only drug approved by the US FDA for treatment of acute ischemic stroke. However, there is significant debate concerning its effectiveness in ischemic stroke. For

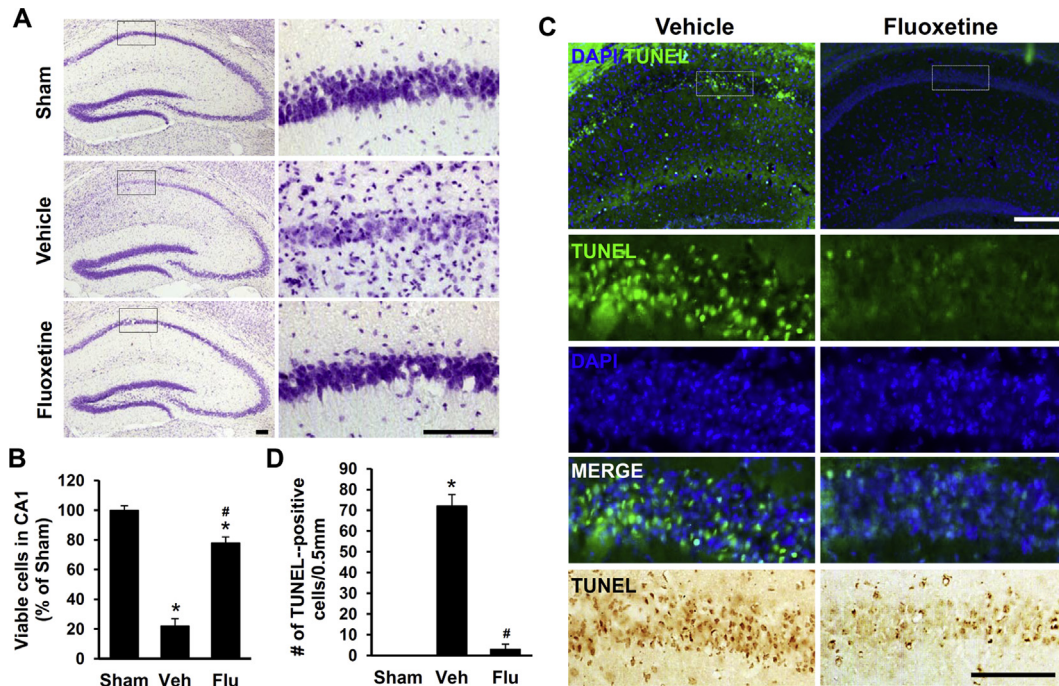


Fig. 7. Fluoxetine inhibits hippocampal cell loss after transient global ischemia. At 7 d after injury, brain tissues from sham, vehicle-treated, and fluoxetine-treated mice were prepared and stained with Cresyl violet and TUNEL-stained as described in the Method. (A) Representative photomicrographs of Nissl staining of the hippocampus. Right panel shows high power views of CA1 area (rectangular boxes in left panel). Scale bars, 100 μ m. (B) Quantification of viable cells in CA1 area. (C) Representative images of TUNEL staining at 7 d after ischemia. Scale bars, 100 μ m. Lower panel shows high power views of CA1 area (dotted boxes in upper panel). (D) Quantitative analysis of TUNEL-positive cells ($n = 3$). Quantitative analysis shows that fluoxetine significantly decreased the number of TUNEL-positive hippocampal neuron in CA1 area after ischemia as compared to vehicle control. Data represent as means \pm SD. * $p < 0.05$ vs. sham group; # $p < 0.05$, vs. vehicle-treated ischemic control group.

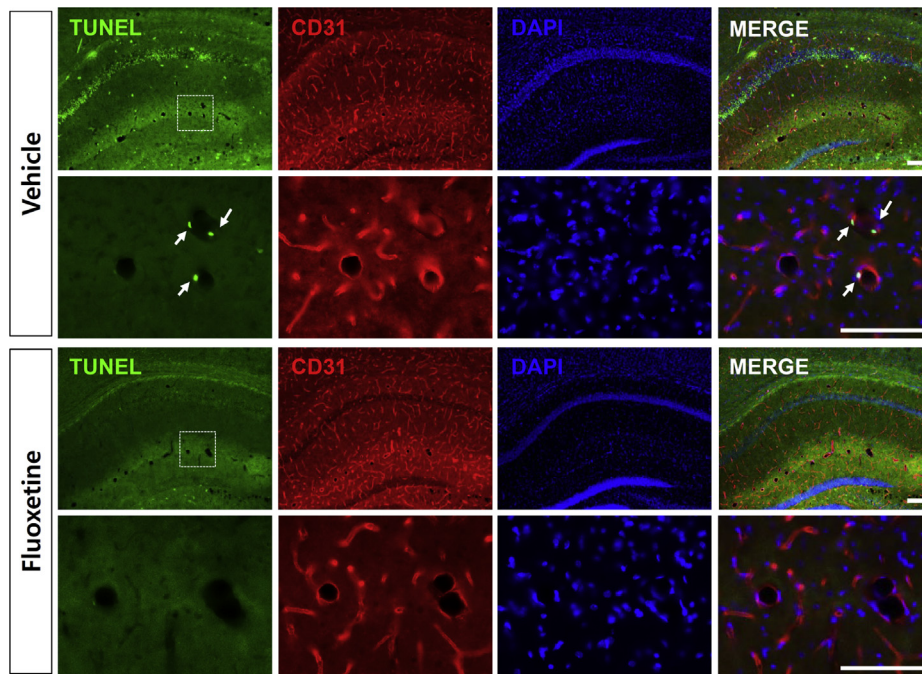


Fig. 8. Fluoxetine also inhibits apoptotic cell death in blood vessel after transient global ischemia. After ischemia, mice were treated with fluoxetine and brain tissues were prepared for TUNEL staining as described in the Method. Some TUNEL stained brain tissues were further labeled with CD31 antibody, a marker of blood vessel endothelial cells. Representative images of double labeling show that CD31-positive signal (red fluorescence) is co-localized with TUNEL-positive cells in the blood vessel (green fluorescence) at 7 d after injury. Lower panels of vehicle and fluoxetine show high power views of dotted boxes (lacunosum-molecular layer) in upper panels of vehicle and fluoxetine. Arrows indicate TUNEL-positive endothelial cells of blood vessels. Note that TUNEL- and CD31-positive cells were not observed in the fluoxetine-treated group. Scale bars, 50 μ m. (For interpretation of the references to color in this figure legend, the reader is referred to the web version of this article.)

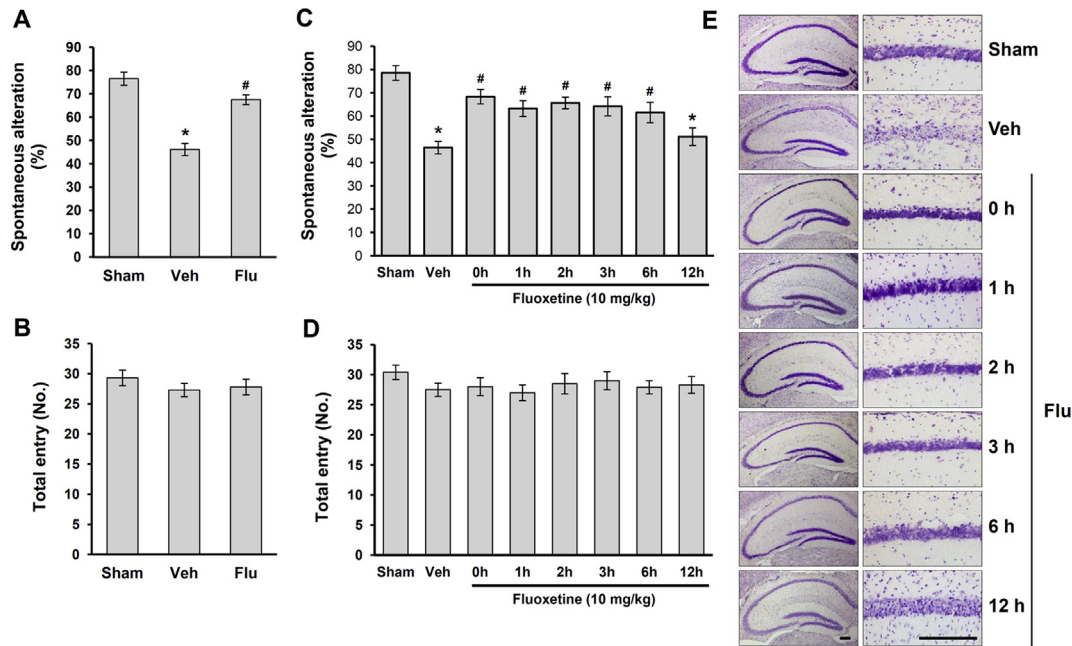


Fig. 9. Fluoxetine improves transient global ischemia-induced memory deficits in the Y-maze task. Mice received transient global ischemia were treated with fluoxetine (10 mg/kg) at indicated time points for 7 d once per day. The final administration was performed 1 h before the behavioral task. Y-maze task was conducted at 7 d after injury. **(A, C)** Spontaneous alteration behavior. **(B, D)** Number of arm entries. Data represent means \pm SD ($n = 10$). * $p < 0.05$ vs. sham group; # $p < 0.05$, vs. vehicle-treated ischemic control group. **(E)** Representative photomicrographs of Nissl staining of the hippocampus. Right panel shows high power views of CA1 area. Scale bars, 200 μ m.

examples, the efficacy and safety of tPA are limited by its narrow treatment time window: it must be administered within 3 h of the onset of symptoms and side effects on brain edema and hemorrhagic complications (Derex and Nighoghossian, 2008; Cronin, 2010). Evidence also shows that tPA induces activation of MMPs after ischemic injury (Adibhatla and Hatcher, 2008). Thus, activation of MMPs by tPA increases its side effects by further disrupting BBB integrity, thereby exacerbating brain edema and cerebral hemorrhage (Adibhatla and Hatcher, 2008). As such, the use of tPA may be contraindicated in hemorrhagic stroke and head trauma. Therefore, additional combination therapies blocking MMPs activation may be required to offset side effects of tPA (Jin et al., 2010). In this regards, fluoxetine can be an excellent candidate for counteracting tPA side effects on MMPs activation and BBB disruption. Furthermore, fluoxetine can be effectively applied for wide treatment time window since BBB breakdown proceeds for prolonged periods in ischemic stroke.

In conclusion, the present study examined the neuroprotective effect of fluoxetine in the mouse model of transient global ischemia. Our study shows that fluoxetine attenuated BBB disruption by reducing MMPs activation and hippocampal neuronal death, leading to alleviating memory and learning impairment after ischemia. As a possible mechanism for preventing BBB damage, thereby reducing neuronal damage by fluoxetine, the inhibitory effect of MMP-2 and -9 expressions by fluoxetine can be considered. Thus, we will further investigate the epigenetic regulation for MMPs expression as a future study. In addition, fluoxetine is currently used as an anti-depressant drug and its safety is proven. Thus, our results suggest that fluoxetine may be used as a therapeutic agent for preserving BBB integrity in ischemic stroke. In this regard, a recent report shows that fluoxetine improves motor recovery after acute ischemic stroke in patients (Chollet et al., 2011).

5. Conflict of interest

The authors declare no conflict of interest.

Acknowledgments

This research was supported by National Research Foundation of Korea funded by the Ministry of Science, ICT & Future Planning [No. 2010-0019349 (Pioneer Research Center Program), No. 2008-0061888 (SRC)].

References

- Abbott, N.J., Ronnback, L., Hansson, E., 2006. Astrocyte-endothelial interactions at the blood-brain barrier. *Nat. Rev. Neurosci.* 7, 41–53.
- Adibhatla, R.M., Hatcher, J.F., 2008. Tissue plasminogen activator (tPA) and matrix metalloproteinases in the pathogenesis of stroke: therapeutic strategies. *CNS Neurol. Disord. Drug Targets* 7, 243–253.
- Anjaneyulu, M., Chopra, K., 2006. Possible involvement of cholinergic and opioid receptor mechanisms in fluoxetine mediated antinociception response in streptozotocin-induced diabetic mice. *Eur. J. Pharmacol.* 538, 80–84.
- Asahi, M., Asahi, K., Jung, J.C., del Zoppo, G.J., Fini, M.E., Lo, E.H., 2000. Role for matrix metalloproteinase 9 after focal cerebral ischemia: effects of gene knockout and enzyme inhibition with BB-94. *J. Cereb. Blood Flow Metab.* 20, 1681–1689.
- Asahi, M., Wang, X., Mori, T., Sumii, T., Jung, J.C., Moskowitz, M.A., Fini, M.E., Lo, E.H., 2001. Effects of matrix metalloproteinase-9 gene knock-out on the proteolysis of blood-brain barrier and white matter components after cerebral ischemia. *J. Neurosci.* 21, 7724–7732.
- Bauer, A.T., Burgers, H.F., Rabie, T., Marti, H.H., 2010. Matrix metalloproteinase-9 mediates hypoxia-induced vascular leakage in the brain via tight junction rearrangement. *J. Cereb. Blood Flow Metab.* 30, 837–848.
- Baumann, E., Preston, E., Slinn, J., Stanimirovic, D., 2009. Post-ischemic hypothermia attenuates loss of the vascular basement membrane proteins, agrin and SPARC, and the blood-brain barrier disruption after global cerebral ischemia. *Brain Res.* 1269, 185–197.
- Begovic, A., Zulic, I., Becic, F., 2004. Testing of analgesic effect of fluoxetine. *Bosn. J. Basic Med. Sci.* 4, 79–81.
- Chen, X., Lan, X., Roche, I., Liu, R., Geiger, J.D., 2008. Caffeine protects against MPTP-induced blood-brain barrier dysfunction in mouse striatum. *J. Neurochem.* 107, 1147–1157.
- Chollet, F., Tardy, J., Albuher, J.F., Thalamos, C., Berard, E., Lamy, C., Bejot, Y., Deltour, S., Jaillard, A., Niclot, P., Guillon, B., Moulin, T., Marque, P., Pariente, J., Arnaud, C., Loubinoux, I., 2011. Fluoxetine for motor recovery after acute ischaemic stroke (FLAME): a randomised placebo-controlled trial. *Lancet Neurol.* 10, 123–130.
- Chung, Y.C., Kim, S.R., Park, J.Y., Chung, E.S., Park, K.W., Won, S.Y., Bok, E., Jin, M., Park, E.S., Yoon, S.H., Ko, H.W., Kim, Y.S., Jin, B.K., 2011. Fluoxetine prevents

- MPTP-induced loss of dopaminergic neurons by inhibiting microglial activation. *Neuropharmacology* 60, 963–974.
- Cronin, C.A., 2010. Intravenous tissue plasminogen activator for stroke: a review of the ECASS III results in relation to prior clinical trials. *J. Emerg. Med.* 38, 99–105.
- Cui, L., Zhang, X., Yang, R., Wang, L., Liu, L., Li, M., Du, W., 2010. Neuroprotection of early and short-time applying atorvastatin in the acute phase of cerebral ischemia: down-regulated 12/15-LOX, p38MAPK and cPLA2 expression, ameliorated BBB permeability. *Brain Res.* 1325, 164–173.
- Dere, L., Nighoghossian, N., 2008. Intracerebral haemorrhage after thrombolysis for acute ischaemic stroke: an update. *J. Neurol. Neurosurg. Psychiatry* 79, 1093–1099.
- Fujimoto, M., Takagi, Y., Aoki, T., Hayase, M., Marumo, T., Gomi, M., Nishimura, M., Kataoka, H., Hashimoto, N., Nozaki, K., 2008. Tissue inhibitor of metalloproteinases protect blood-brain barrier disruption in focal cerebral ischemia. *J. Cereb. Blood Flow Metab.* 28, 1674–1685.
- Gerzanich, V., Woo, S.K., Vennekens, R., Tsybalyuk, O., Ivanova, S., Ivanov, A., Geng, Z., Chen, Z., Nilius, B., Flockner, V., Freichel, M., Simard, J.M., 2009. De novo expression of Trpm4 initiates secondary hemorrhage in spinal cord injury. *Nat. Med.* 15, 185–191.
- Hartung, H.P., Kieser, B.C., 2000. The role of matrix metalloproteinases in autoimmune damage to the central and peripheral nervous system. *J. Neuroimmunol.* 107, 140–147.
- Hawkins, B.T., Davis, T.P., 2005. The blood-brain barrier/neurovascular unit in health and disease. *Pharmacol. Rev.* 57, 173–185.
- Higashida, T., Kreipke, C.W., Rafols, J.A., Peng, C., Schafer, S., Schafer, P., Ding, J.Y., Dornbos III, D., Li, X., Guthikonda, M., Rossi, N.F., Ding, Y., 2011. The role of hypoxia-inducible factor-1 α , aquaporin-4, and matrix metalloproteinase-9 in blood-brain barrier disruption and brain edema after traumatic brain injury. *J. Neurosurg.* 114, 92–101.
- Hosokawa, T., Nakajima, H., Doi, Y., Sugino, M., Kimura, F., Hanafusa, T., Takahashi, T., 2011. Increased serum matrix metalloproteinase-9 in neuromyelitis optica: implication of disruption of blood-brain barrier. *J. Neuroimmunol.* 236, 81–86.
- Jin, R., Yang, G., Li, G., 2010. Molecular insights and therapeutic targets for blood-brain barrier disruption in ischemic stroke: critical role of matrix metalloproteinases and tissue-type plasminogen activator. *Neurobiol. Dis.* 38, 376–385.
- Jin, Y.J., Park, I., Hong, I.K., Byun, H.J., Choi, J., Kim, Y.M., Lee, H., 2011. Fibronectin and vitronectin induce AP-1-mediated matrix metalloproteinase-9 expression through integrin $\alpha(5)\beta(1)/\alpha(v)\beta(3)$ -dependent Akt, ERK and JNK signaling pathways in human umbilical vein endothelial cells. *Cell Signal* 23, 125–134.
- Kim, D.H., Kim, S., Jung, W.Y., Park, S.J., Park, D.H., Kim, J.M., Cheong, J.H., Ryu, J.H., 2009. The neuroprotective effects of the seeds of *Cassia obtusifolia* on transient cerebral global ischemia in mice. *Food Chem. Toxicol.* 47, 1473–1479.
- Kirino, T., 2000. Delayed neuronal death. *Neuropathology* 20 (Suppl.), S95–S97.
- Kirino, T., 1982. Delayed neuronal death in the gerbil hippocampus following ischemia. *Brain Res.* 239, 57–69.
- Lakhan, S.E., Kirchgessner, A., Hofer, M., 2009. Inflammatory mechanisms in ischemic stroke: therapeutic approaches. *J. Transl. Med.* 7, 97.
- Lakhan, S.E., Kirchgessner, A., Tepper, D., Leonard, A., 2013. Matrix metalloproteinases and blood-brain barrier disruption in acute ischemic stroke. *Front Neurol.* 4, 32.
- Lee, H., Park, J.W., Kim, S.P., Lo, E.H., Lee, S.R., 2009. Doxycycline inhibits matrix metalloproteinase-9 and laminin degradation after transient global cerebral ischemia. *Neurobiol. Dis.* 34, 189–198.
- Lee, J.Y., Kim, H.S., Choi, H.Y., Oh, T.H., Yune, T.Y., 2012. Fluoxetine inhibits matrix metalloproteinase activation and prevents disruption of blood-spinal cord barrier after spinal cord injury. *Brain* 135, 2375–2389.
- Lee, S.R., Tsuji, K., Lee, S.R., Lo, E.H., 2004. Role of matrix metalloproteinases in delayed neuronal damage after transient global cerebral ischemia. *J. Neurosci.* 24, 671–678.
- Lim, C.M., Kim, S.W., Park, J.Y., Kim, C., Yoon, S.H., Lee, J.K., 2009. Fluoxetine affords robust neuroprotection in the postischemic brain via its anti-inflammatory effect. *J. Neurosci. Res.* 87, 1037–1045.
- Lipton, P., 1999. Ischemic cell death in brain neurons. *Physiol. Rev.* 79, 1431–1568.
- Liu, S., Agalliu, D., Yu, C., Fisher, M., 2012. The role of pericytes in blood-brain barrier function and stroke. *Curr. Pharm. Des.* 18, 3653–3662.
- Lo, E.H., Wang, X., Cuzner, M.L., 2002. Extracellular proteolysis in brain injury and inflammation: role for plasminogen activators and matrix metalloproteinases. *J. Neurosci. Res.* 69, 1–9.
- Miyazaki, K., Ohta, Y., Nagai, M., Morimoto, N., Kurata, T., Takehisa, Y., Ikeda, Y., Matsuura, T., Abe, K., 2011. Disruption of neurovascular unit prior to motor neuron degeneration in amyotrophic lateral sclerosis. *J. Neurosci. Res.* 89, 718–728.
- Mun-Bryce, S., Rosenberg, G.A., 1998. Matrix metalloproteinases in cerebrovascular disease. *J. Cereb. Blood Flow Metab.* 18, 1163–1172.
- Noble, L.J., Donovan, F., Igarashi, T., Goussev, S., Werb, Z., 2002. Matrix metalloproteinases limit functional recovery after spinal cord injury by modulation of early vascular events. *J. Neurosci.* 22, 7526–7535.
- Okuyama, S., Minami, S., Shimada, N., Makihata, N., Nakajima, M., Furukawa, Y., 2013. Anti-inflammatory and neuroprotective effects of auraptene, a citrus coumarin, following cerebral global ischemia in mice. *Eur. J. Pharmacol.* 699, 118–123.
- Preston, E., Webster, J., 2004. A two-hour window for hypothermic modulation of early events that impact delayed opening of the rat blood-brain barrier after ischemia. *Acta Neuropathol.* 108, 406–412.
- Pulsinelli, W.A., Brierley, J.B., Plum, F., 1982. Temporal profile of neuronal damage in a model of transient forebrain ischemia. *Ann. Neurol.* 11, 491–498.
- Ramos-Fernandez, M., Bellolio, M.F., Stead, L.G., 2011. Matrix metalloproteinase-9 as a marker for acute ischemic stroke: a systematic review. *J. Stroke Cerebrovasc. Dis.* 20, 47–54.
- Rosenberg, G.A., 2002. Matrix metalloproteinases in neuroinflammation. *Glia* 39, 279–291.
- Rosenberg, G.A., Dencoff, J.E., McGuire, P.G., Liotta, L.A., Stetler-Stevenson, W.G., 1994. Injury-induced 92-kilodalton gelatinase and urokinase expression in rat brain. *Lab. Invest.* 71, 417–422.
- Rosenberg, G.A., Estrada, E.Y., Dencoff, J.E., 1998. Matrix metalloproteinases and TIMPs are associated with blood-brain barrier opening after reperfusion in rat brain. *Stroke* 29, 2189–2195.
- Rosenberg, G.A., Estrada, E.Y., Dencoff, J.E., Stetler-Stevenson, W.G., 1995. Tumor necrosis factor- α -induced gelatinase B causes delayed opening of the blood-brain barrier: an expanded therapeutic window. *Brain Res.* 703, 151–155.
- Rosenberg, G.A., Navratil, M., 1997. Metalloproteinase inhibition blocks edema in intracerebral hemorrhage in the rat. *Neurology* 48, 921–926.
- Sairanen, T.R., Lindsberg, P.J., Brenner, M., Carpen, O., Siren, A., 2001. Differential cellular expression of tumor necrosis factor- α and Type I tumor necrosis factor receptor after transient global forebrain ischemia. *J. Neurol. Sci.* 186, 87–99.
- Sakurai-Yamashita, Y., Shigematsu, K., Yamashita, K., Niwa, M., 2006. Expression of MCP-1 in the hippocampus of SHRSP with ischemia-related delayed neuronal death. *Cell Mol. Neurobiol.* 26, 823–831.
- Sounvoravong, S., Nakashima, M.N., Wada, M., Nakashima, K., 2007. Modification of antiallostatic and antinociceptive effects of morphine by peripheral and central action of fluoxetine in a neuropathic mice model. *Acta Biol. Hung.* 58, 369–379.
- Sternlicht, M.D., Lochter, A., Sympon, C.J., Huey, B., Rougier, J.P., Gray, J.W., Pinkel, D., Bissell, M.J., Werb, Z., 1999. The stromal proteinase MMP3/stromelysin-1 promotes mammary carcinogenesis. *Cell* 98, 137–146.
- Sternlicht, M.D., Werb, Z., 2001. How matrix metalloproteinases regulate cell behavior. *Annu. Rev. Cell Dev. Biol.* 17, 463–516.
- Tulsulkar, J., Shah, Z.A., 2013. Ginkgo biloba prevents transient global ischemia-induced delayed hippocampal neuronal death through antioxidant and anti-inflammatory mechanism. *Neurochem. Int.* 62, 189–197.
- Utepergenov, D.I., Mertsch, K., Sporbart, A., Tenz, K., Paul, M., Haseloff, R.F., Blasig, I.E., 1998. Nitric oxide protects blood-brain barrier in vitro from hypoxia/reoxygenation-mediated injury. *FEBS Lett.* 424, 197–201.
- Wang, X., Jung, J., Asahi, M., Chwang, W., Russo, L., Moskowitz, M.A., Dixon, C.E., Fini, M.E., Lo, E.H., 2000. Effects of matrix metalloproteinase-9 gene knock-out on morphological and motor outcomes after traumatic brain injury. *J. Neurosci.* 20, 7037–7042.
- Werb, Z., 1997. ECM and cell surface proteolysis: regulating cellular ecology. *Cell* 91, 439–442.
- Xu, J., Kim, G.M., Ahmed, S.H., Xu, J., Yan, P., Xu, X.M., Hsu, C.Y., 2001. Glucocorticoid receptor-mediated suppression of activator protein-1 activation and matrix metalloproteinase expression after spinal cord injury. *J. Neurosci.* 21, 92–97.
- Xuan, A., Long, D., Li, J., Ji, W., Hong, L., Zhang, M., Zhang, W., 2012. Neuroprotective effects of valproic acid following transient global ischemia in rats. *Life Sci.* 90, 463–468.
- Yang, D.Y., Pan, H.C., Chen, C.J., Cheng, F.C., Wang, Y.C., 2007a. Effects of tissue plasminogen activator on cerebral microvessels of rats during focal cerebral ischemia and reperfusion. *Neurol. Res.* 29, 274–282.
- Yang, Y., Estrada, E.Y., Thompson, J.F., Liu, W., Rosenberg, G.A., 2007b. Matrix metalloproteinase-mediated disruption of tight junction proteins in cerebral vessels is reversed by synthetic matrix metalloproteinase inhibitor in focal ischemia in rat. *J. Cereb. Blood Flow Metab.* 27, 697–709.
- Yong, C., Arnold, P.M., Zoubine, M.N., Citron, B.A., Watanabe, I., Berman, N.E., Festoff, B.W., 1998. Apoptosis in cellular compartments of rat spinal cord after severe contusion injury. *J. Neurotrauma* 15, 459–472.
- Yu, F., Kamada, H., Niizuma, K., Endo, H., Chan, P.H., 2008. Induction of mmp-9 expression and endothelial injury by oxidative stress after spinal cord injury. *J. Neurotrauma* 25, 184–195.
- Zhen, G., Dore, S., 2007. Optimized protocol to reduce variable outcomes for the bilateral common carotid artery occlusion model in mice. *J. Neurosci. Methods* 166, 73–80.
- Zlokovic, B.V., 2008. The blood-brain barrier in health and chronic neurodegenerative disorders. *Neuron* 57, 178–201.